

BRIGHTENING X-RAY EMISSION FROM GW170817/GRB170817A:  
FURTHER EVIDENCE FOR AN OUTFLOW

JOHN J. RUAN,<sup>1</sup> MELANIA NYNKA,<sup>1</sup> DARYL HAGGARD,<sup>1,2</sup> VICKY KALOGERA,<sup>3</sup> AND PHIL EVANS<sup>4</sup>

<sup>1</sup>*McGill Space Institute and Department of Physics, McGill University, 3600 rue University, Montreal, Quebec, H3A 2T8, Canada*

<sup>2</sup>*CIFAR Azrieli Global Scholar, Gravity & the Extreme Universe Program, Canadian Institute for Advanced Research, 661 University Avenue, Suite 505, Toronto, ON M5G 1M1, Canada*

<sup>3</sup>*Center for Interdisciplinary Exploration and Research in Astrophysics and Department of Physics and Astronomy, Northwestern University, 2145 Sheridan Road, Evanston, Illinois 60208-3112, USA*

<sup>4</sup>*Leicester Institute for Space and Earth Observation and Department of Physics & Astronomy, University of Leicester, University Road, Leicester, LE1 7RH, UK*

(Received December 7, 2017)

Submitted to ApJ Letters

ABSTRACT

The origin of the X-ray emission from neutron star coalescence GW170817/GRB170817A is a key diagnostic of the unsettled post-merger narrative, and different scenarios predict distinct evolution in its X-ray light curve. Due to its sky proximity to the Sun, sensitive X-ray monitoring of GW170817/GRB170817A has not been possible since a previous detection at 16 days post-burst. We present new, deep *Chandra* observations of GW170817/GRB170817A at 109 days post-burst, immediately after Sun constraints were lifted. The X-ray emission has brightened to a flux of  $F_{0.3-8 \text{ keV}} = 15.8 \times 10^{-15} \text{ erg s}^{-1} \text{ cm}^{-2}$ , at a similar rate to the radio light curve. This confirms that the X-ray and radio emission have a common origin. We show that the X-ray light curve is consistent with outflow models based on radio observations. The outflow in these models may be either a cocoon shocked by the jet or dynamical ejecta from the merger. Further deep X-ray monitoring can place powerful constraints on the physical parameters of these models, by both timing the passing of a synchrotron cooling break through the X-ray band, and detecting the associated steepening of the X-ray photon index. Finally, the X-ray brightening strengthens the argument that simple top-hat jet models are not consistent with the latest observations. However, more advanced models of structured jets with off-axis viewing angles should be pursued and cannot yet be ruled out.

*Keywords:* gravitational waves: individual (GW170817); gamma-ray burst: individual (GRB170817A); stars: neutron; X-rays: binaries

arXiv:1712.02809v2 [astro-ph.HE] 11 Dec 2017

## 1. INTRODUCTION

The gravitational wave (GW) and multi-wavelength electromagnetic (EM) discoveries of the binary neutron star (NS) merger GW170817 marked the dawn of multi-messenger GW astronomy (e.g., Abbott et al. 2017a,b; Coulter et al. 2017; Evans et al. 2017; Goldstein et al. 2017; Hallinan et al. 2017; Soares-Santos et al. 2017; Troja et al. 2017; Valenti et al. 2017). Detection of the short Gamma-ray burst (sGRB) GRB170817A associated with the gravitational wave event GW170817 confirmed that binary NS mergers are the progenitors of at least some sGRBs (Abbott et al. 2017c; Goldstein et al. 2017; Savchenko et al. 2017). Furthermore, observations of the optical and infrared transient confirmed that binary NS mergers produce kilonova, powered by r-process nucleosynthesis (Arcavi et al. 2017; Cowperthwaite et al. 2017; Drout et al. 2017; Kasliwal et al. 2017; McCully et al. 2017; Pian et al. 2017; Shappee et al. 2017; Smartt et al. 2017). Finally, robust association of GW170817 with its host galaxy (Hjorth et al. 2017; Im et al. 2017; Levan et al. 2017) enabled measurements of the Hubble constant independent of the cosmic distance ladder (Abbott et al. 2017d; Guidorzi et al. 2017), providing a new probe of cosmology. However, many questions about the nature of GW170817 remain open.

X-ray observations of GW170817 provided important early indication that the associated sGRB GRB170817A was unlike any other GRB afterglow previously observed. *Chandra* observations of the optical counterpart (SSS17a; Coulter et al. 2017) at  $\sim 2$  days post-burst yielded a non-detection (Margutti et al. 2017). However, *Chandra* observations at  $\sim 9$  days post-burst revealed a new X-ray source coincident with the position of the optical transient (Troja et al. 2017). This delayed brightening of the X-ray counterpart has not been observed in standard GRB afterglows, which instead display consistent dimming in their X-ray light curves on timescales of days. The discovery of an X-ray counterpart was confirmed in additional *Chandra* observations at  $\sim 15$  and 16 days post-burst, which surprisingly showed that the source had not dimmed significantly (Haggard et al. 2017). Unfortunately, Sun-constraints prevented further X-ray monitoring of GRB170817A after the last detection at 16 days post-burst, until early December 2017 ( $\sim 109$  days post-burst).

The origin of the observed X-ray emission from GRB170817A is still unclear. Haggard et al. (2017), Margutti et al. (2017), and Troja et al. (2017) all showed that the *Chandra* X-ray light curve is consistent with the fading of a standard sGRB afterglow in which the jet is off-axis from the line of sight by  $20\text{-}30^\circ$ . This interpretation is ostensibly supported by the low fluence observed

in the prompt  $\gamma$ -ray emission (e.g., Abbott et al. 2017c; Fong et al. 2017; Goldstein et al. 2017; Murguia-Berthier et al. 2017), which was a factor of  $\sim 10^3$  lower than previously observed in any other sGRBs. Modeling of the radio light curves of GRB170817A similarly showed consistency with off-axis sGRB afterglows (Alexander et al. 2017; Hallinan et al. 2017). If confirmed, this also makes GRB170817A the first off-axis sGRB ever observed, but other interpretations for the X-ray emission are not ruled out.

Alternatively, is it possible that the X-ray emission from GRB170817A is from the afterglow of a mildly-relativistic cocoon. Hydrodynamic simulations of GRB jets have shown that as the jet travels through the ejecta surrounding the burst, the jet head will shock the debris and produce a hot cocoon around the jet (Gottlieb et al. 2018; Lazzati et al. 2017; Nakar & Piran 2017). This cocoon can be mildly-relativistic, and shock the external medium after breakout to produce synchrotron afterglow emission in X-rays that is observable over a wide range of viewing-angles. Early evidence for a cocoon in GRB170817A was provided by the soft thermal tail observed in the  $\gamma$ -ray light curve of its prompt emission, which can be produced by cooling emission from a cocoon (Goldstein et al. 2017). Piro & Kollmeier (2017) also showed that the early blue emission of the optical transient associated with GRB170817A is consistent with shock cooling in a cocoon.

More recently, Mooley et al. (2017) showed that the late-time radio light curve of GRB170817A supports an outflow afterglow interpretation for the origin of the radio emission. In these models, the outflow could either be a mildly-relativistic cocoon that is produced by a choked jet, or the high-velocity tail of the dynamical ejecta from the neutron star coalescence. Mooley et al. (2017) show that the observed slow brightening in the radio light curve up to 93 days post-burst requires an outflow in which the majority of the kinetic energy of the blast-wave is in the lower-velocity material. This leads to a continuous injection of energy into the shock, and thus a slow, monotonic rise of the afterglow emission. In these outflow models, an observable jet that breaks out of the ejecta is not required (or even favored). Furthermore, Mooley et al. (2017) rule out simple off-axis GRB models for the origin of the radio emission, which fail to reproduce the slowly-brightening radio light curve.

The late-time X-ray light curve of GRB170817A can provide critical evidence to test our rapidly-evolving understanding of the EM transient. An X-ray light curve that brightens as the radio emission has done, can confirm that the radio and X-ray emission have a common origin. This X-ray brightening would also provide ev-

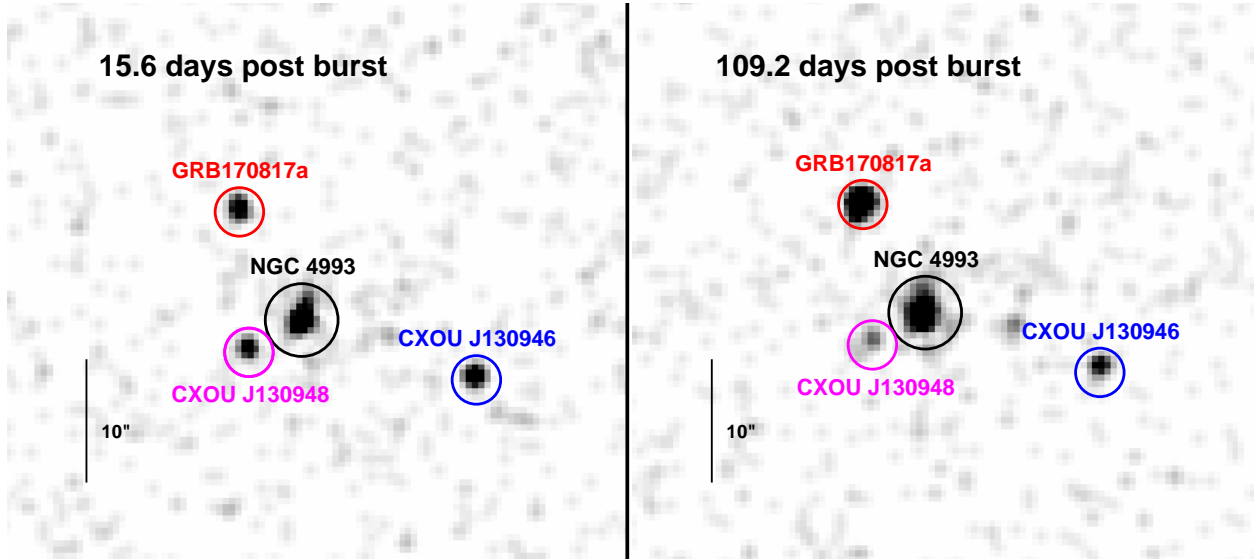


**Figure 1.** *Left:* *Chandra* 0.5 – 8.0 keV X-ray image of GRB170817A at 15.6 days post-burst, in a 93.4 ks observation from Haggard et al. (2017). X-ray emission from GRB170817A is clearly detected, along with the host-galaxy NGC 4993 and two other sources in the field. *Chandra* observations beyond this observations were Sun-constrained until early December 2017. *Right:* A subsequent 98.8 ks *Chandra* image at  $\sim 109.2$  days post-burst, immediately after Sun constraints were lifted. The X-ray emission from GRB170817A is still detected and has brightened. All images are shown in linear scale, smoothed with a 2-pixel Gaussian kernel.

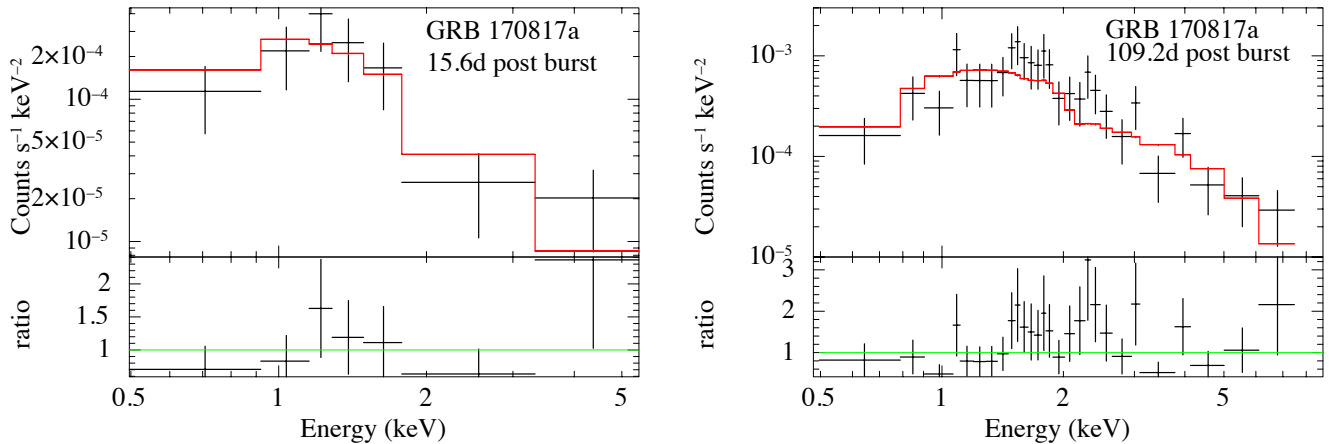


**Figure 2.** *Chandra* co-added X-ray spectra from GRB170817A in a 93.4 ks exposure at 15.6 days (*Left*) and a 98.8 ks exposure at 109.2 days post-burst (*Right*). Spectral data and residuals are shown in black and the best-fit spectral models are in red. The neutral hydrogen absorption column is fixed to  $N_{\text{H}} = 7.5 \times 10^{20} \text{ cm}^{-2}$  (see Section 2). These spectra at 15.6 and 109.2 days each consist of two exposures that were jointly fit. In the joint fit for each epoch, the spectral index  $\Gamma$  was tied between the exposures while the power-law normalization was left free.

idence that the X-ray emission is the afterglow of an outflow, as suggested by radio observations. Furthermore, deep X-ray observations can determine the origin of the outflow by constraining its velocity, based on the time at which a synchrotron cooling break is observed to pass through the X-ray band.

In this Letter, we present deep *Chandra* observations of GRB170817A at 109.2 days post-burst. Due to Sun constraints, these are the first X-ray observations since

the previous *Chandra* detection at 16 days post-burst. The outline of this Letter is as follows: In Section 2, we describe our *Chandra* observations and data reduction procedure. In Section 3, we discuss the origin of the X-ray and radio emission, and compare the observed X-ray light curve to predictions from outflow afterglow models based on radio observations. We briefly summarize and conclude in Section 4.

**Table 1.** X-ray Source Properties at 15.6 days and 109.2 Days Post-Burst

Source	RA	Dec	Days	Power Law	Flux (0.3 – 8 keV)	Luminosity (0.3 – 10 keV) <sup>a,b</sup>
ID	(J2000)	(J2000)	Post-Burst	$\Gamma$	[ $10^{-14}$ erg s $^{-1}$ cm $^{-2}$ ]	[ $10^{38}$ erg s $^{-1}$ ]
GRB170817A	13:09:48.077	-23:22:53.459	15.6	$2.4^{+0.8}_{-0.8}$	$0.36^{+0.1}_{-0.07}$	$10.4^{+2.0}_{-1.6}$
			109.2	$1.62^{+0.27}_{-0.26}$	$1.58^{+0.14}_{-0.13}$	$42.5^{+3.7}_{-3.5}$
CXOU J130948	13:09:48.014	-23:23:04.917	15.6	$1.3^{+0.8}_{-0.8}$	$0.4^{+0.1}_{-0.09}$	$10.8^{+4.4}_{-2.4}$
			109.2	$2.4 \pm 1.7$	$0.2^{+0.3}_{-0.1}$	$6.5^{+9.9}_{-4.7}$
CXOU J130946	13:09:46.682	-23:23:06.983	15.6	$-0.4^{+0.2}_{-0.8}$	$1.1^{+0.1}_{-0.1}$	$38.8^{+4.0}_{-9.8}$
			109.2	$0.4 \pm 0.9$	$0.5^{+0.5}_{-0.3}$	$17.5^{+11.9}_{-10.3}$
NGC 4993	13:09:47.705	-23:23:02.457	15.6	$1.5^{+0.4}_{-0.4}$	$1.3 \pm 0.2$	$34.8^{+3.2}_{-3.6}$
			109.2	$1.4^{+0.4}_{-0.3}$	$1.4 \pm 0.2$	$38.9^{+5.8}_{-5.4}$

NOTE—All reported errors represent 90% confidence intervals. The neutral hydrogen absorption was frozen to  $N_{\text{H}} = 7.5 \times 10^{20}$  cm $^{-2}$  for all spectral fits, based on NGC 4993’s  $A_{\text{V}} = 0.338$  (Schlafly & Finkbeiner 2011).

<sup>a</sup> A luminosity distance of 42.5 Mpc was assumed for all sources.

<sup>b</sup> The luminosities at 15.6 days listed here are larger than reported in Haggard *et al.* (2017) by a factor of 4, due to a calculation error.

## 2. X-RAY OBSERVATIONS AND ANALYSIS

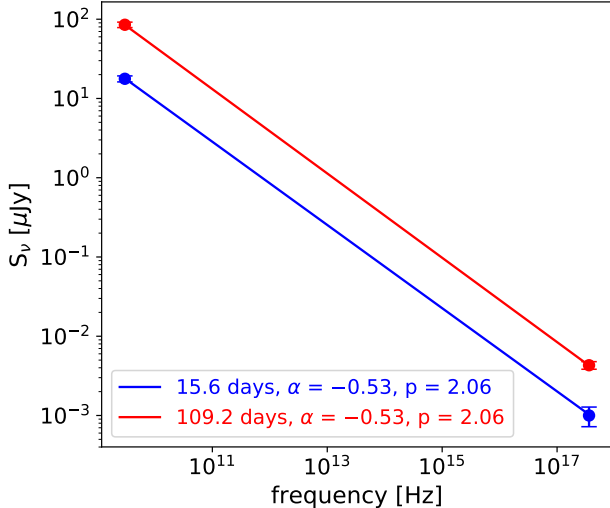
New X-ray observations of GRB170817A were obtained via a *Chandra* Director’s Discretionary Time allocation (PI: Wilkes, Program Number 18408601). This program obtained two exposures of GRB170817A: (1) a 74.09 ks exposure (ObsID 20860) beginning at 2017 December 2.08 UT, approximately 108 days post-burst, and (2) a 24.74 ks exposure (ObsID 20861) beginning at 2017 December 6.45 UT, approximately 111 days post-burst. Both these exposures were acquired using *Chandra*’s ACIS-S3 chip in VFAINT mode. We use CIAO v.4.9 (CALDB v4.7.6; Fruscione *et al.* 2006) for reduction and analysis of these X-ray data. We reprocess the level 2 events files and use CIAO’s `repro` script to apply the latest calibrations. Since the two new exposures are close in time and the X-ray emission of GRB170817A is not expected to vary significantly over  $\sim 4$  day timescales, we co-add the two data sets into one 98.83 ks exposure at 109.2 days post-burst.

Figure 1 shows our latest *Chandra* 0.5–8 keV image of GRB170817A at 109.2 days post-burst (*Right*), in comparison to the *Chandra* image from a similar exposure at 15.6 days post-burst from Haggard *et al.* (2017) (*Left*). The previously-detected X-ray source at the position of GRB170817A is still detected in this latest observation, along with the three other previously-detected X-ray sources in the field: CXOU J130948, CXOU 130946, and the host galaxy NGC 4993.

To measure the flux of each of the four sources, we first apply the point-source detection algorithm `wavdetect` to each 0.5 – 7 keV image to determine the centroid positions of each source. Following the same procedure from Haggard *et al.* (2017), we extract spectra from the point sources GRB170817A, CXOU J130948, and CXOU 130946 using extraction regions with radii 1’’97 in size (corresponding to  $\sim 90\%$  encircled energy fraction near the *Chandra* on-axis position). For the host galaxy NGC 4993 we adopt an extraction region with a 2’’95 radius, large enough to include most of the galaxy’s X-ray flux while avoiding contamination from nearby CXOU J130948. These regions are shown in Figure 1. We obtain background photons from a large region on the same chip that does not overlap other sources.

We extract spectra and response files for the four detected X-ray sources using the CIAO `specextract` tool from the individual observations. The resultant files are then co-added to improve statistics. We fit the combined spectra using XSPEC v12.9.0 (Arnaud 1996), with atomic cross sections from Verner *et al.* (1996) and abundances from Wilms *et al.* (2000). For each of the four sources, we assume absorbed power-law spectral models with fixed  $N_{\text{H}} = 7.5 \times 10^{20}$  cm $^{-2}$ . The best-fit power-law spectral indices, absorbed 0.3 – 8 keV fluxes, and 0.3 – 10 keV luminosities are listed in Table 1.

Our X-ray analysis shows that the X-ray flux of GRB170817A has brightened significantly to an ab-



**Figure 3.** Comparison of the radio to X-ray flux densities at 15.6 days (blue points) and 109.2 days post-burst (red points). The X-ray-to-radio spectral index  $\alpha$  remains constant at  $-0.53$  over this timespan, indicating that the X-ray emission brightened at the same rate as the radio.

sorbed flux of  $F_{0.3-8 \text{ keV}} = 15.8 \times 10^{-15} \text{ erg s}^{-1} \text{ cm}^{-2}$  at 109.2 days post-burst, which corresponds to an unabsorbed luminosity of  $L_{0.3-10 \text{ keV}} = 4.3 \times 10^{39} \text{ erg s}^{-1}$ . The extracted X-ray spectrum at 109.2 days is shown in Figure 2, along with our previous spectrum at 15.6 days from Haggard et al. (2017) for comparison. The flux and spectrum of the host-galaxy NGC 4993 and CXOU J130946 are consistent with our previous deep Chandra observations. CXOU J130948 is known to be variable in X-ray, and while our spectral analysis shows its spectrum is consistent with those previously reported, the best-fit parameters are not well constrained. The source is visibly dimmer at 109.2 days (Figure 1) and shows a  $\sim 48\%$  decrease in count rate between the two epochs (Table 1; Margutti et al. 2017; Haggard et al. 2017).

### 3. DISCUSSION

The observed X-ray brightening of GRB170817A at 109.2 days in comparison to previous X-ray observations at 9 and 15.6 days has profound implications for our understanding of the EM transient. In Section 3.1 below, we first test whether the X-ray and radio emission have the same origin, by comparing the X-ray fluxes to the radio observations. We find that the X-rays brightened at a similar rate as the radio emission, confirming that they share a common origin. In Section 3.2, we consider the possibility that both the X-ray and radio emission are due to the afterglow of an outflow, either from a cocoon or dynamical ejecta. We find that the X-ray light curve is well-described by predictions from outflow models based on radio observations.

#### 3.1. Comparison of X-ray and Radio Emission: Evidence for A Common Origin

The similar brightening of both X-ray and radio emission from GRB170817A suggests that the X-ray and radio emission may have a common origin. This can be confirmed if the X-ray-to-radio spectral index  $\alpha$  (where  $S_\nu \sim \nu^\alpha$ ) is measured to be constant between 15.6 and 109.2 days post-burst. In this scenario, the X-ray light curve would be consistent with the results of Mooley et al. (2017), in which afterglow emission from an outflow is the origin of both the radio and X-ray emission, while off-axis GRB afterglows are ruled out. If instead  $\alpha$  is measured to have steepened, this can either indicate that the X-ray and radio emission have different origins, or that they have the same synchrotron origin but a cooling break has passed through the X-ray band.

We compare the X-ray-to-radio spectral index  $\alpha$  at 15.6 and 109.2 days and find that it remains constant, confirming a common origin for both the X-ray and radio emission. For the X-ray, we use the measured X-ray flux densities at 15.6 days from Haggard et al. (2017) and at 109.2 days reported here. For the radio, we use the VLA 3 GHz radio light curve from Hallinan et al. (2017) and Mooley et al. (2017), which covers a timespan from 16.4 to 93.1 days post-burst. Mooley et al. (2017) showed that this radio light curve is well-fit by a power-law with slope  $t^{0.8}$ , and thus we also fit a power-law to extrapolate the radio flux density at 15.6 and 109.2 days. The uncertainties on these two extrapolated radio flux densities are estimated through Monte Carlo resampling of the radio flux density measurements in the light curve based on their uncertainties, then reperforming the fit and extrapolation. Figure 3 compares the X-ray and radio flux densities at the two epochs. The fitted X-ray-to-radio spectral index is  $-0.53 \pm 0.02$  at 15.6 days, and  $-0.53 \pm 0.01$  at 109.2 days. Thus, we detect no change in  $\alpha$ , implying that the X-rays brightened at the same rate as the radio. The similar rate of brightening in the X-ray and radio light curves thus confirms a common origin. Moreover, the consistency between the radio spectral index ( $\alpha = 0.60$ ; Alexander et al. 2017; Mooley et al. 2017) and X-ray photon index we measure ( $\Gamma = 0.62$ , where  $\alpha = \Gamma - 1$ ; see Table 1) further supports this conclusion.

#### 3.2. X-ray Consistency with Outflow Models

Mooley et al. (2017) showed that the brightening radio light curve of GRB170817A is well-described by models of afterglow emission from an outflow. This outflow can be a mildly-relativistic cocoon shocked by the jet head, or the high-velocity tail of dynamical ejecta from the neutron star coalescence. In both cases, the slow and

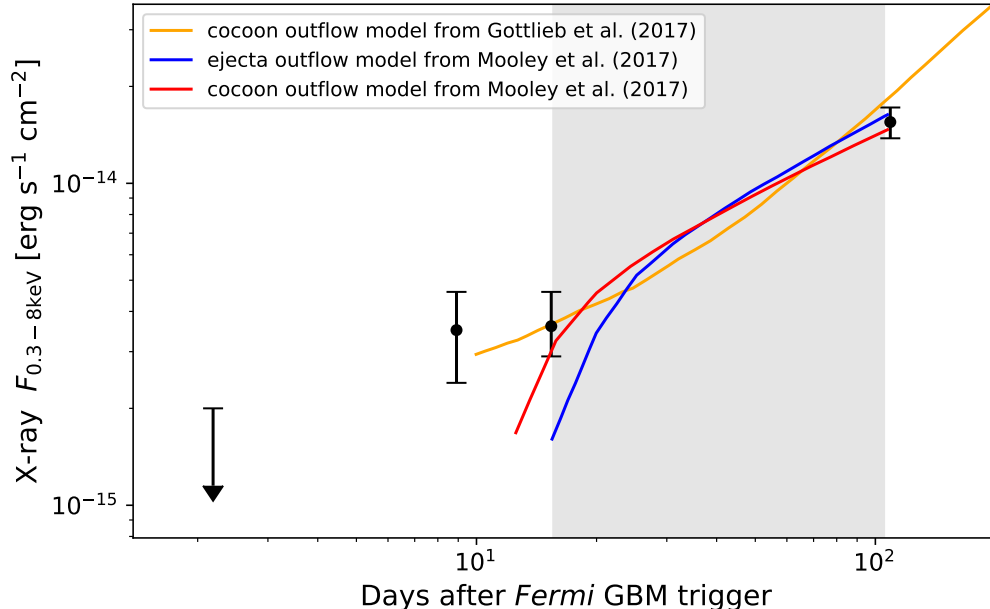


**Figure 4.** *Chandra* X-ray light curve of GRB170817A (black points), including our new observations at 109.2 days post-burst. The predicted X-ray light curves from the cocoon model of Gottlieb et al. (2017) (solid orange line), as well as the cocoon (solid red line) and ejecta (solid blue line) models of Mooley et al. (2017) are also shown. The gray shaded region is the timespan over which *Chandra* observations were not possible due to Sun constraints. The brightening X-ray light curve is well-described by cocoon or dynamical ejecta models, in excellent agreement with radio observations.

monotonic rise of the radio light curve implies that the blast-wave must have a continued injection of kinetic energy. Mooley et al. (2017) show that both cocoon and dynamical ejecta models in which the majority of the kinetic energy is in the lower velocity material provide excellent fits to the radio light curve. These models also predict that the X-ray light curve will rise at the same rate as the radio, which we can directly test with our X-ray light curve.

We produce predicted X-ray light curves based on the radio light curves from both the cocoon and ejecta outflow models presented in Mooley et al. (2017), as well as the cocoon outflow model from Gottlieb et al. (2017). The X-ray emission is estimated by scaling the model radio light curves to the X-rays based on the X-ray-to-radio flux ratio at 15.6 days post-burst. This assumes that the synchrotron cooling break has not yet passed through the X-rays, and thus the X-ray-to-radio spectral index remains constant. This assumption is justified because the fiducial models used by Mooley et al. (2017) to fit the radio light curve predict that the synchrotron cooling frequency is still well above the *Chandra* band at 109.2 days post-burst. The predicted X-ray light curves from these outflow models are shown in Figure 4.

The predicted X-ray light curves from the three outflow models in Figure 4 provide excellent fits to our observed X-ray flux at 109.2 days post-burst. The agreement of these models with both the X-ray and radio light curves supports an outflow afterglow as the source of

both the radio and X-ray emission from GRB170817A, and implies that the synchrotron cooling break has not yet passed through the X-ray band.

If the synchrotron cooling frequency is still above the X-ray band, continued deep *Chandra* observations will provide the first indication of the cooling break, via a change in the X-ray photon index  $\Gamma$ . Across the break frequency, the X-ray photon index should be observed to steepen by  $\Delta\Gamma = 0.5$  (where  $\alpha = \Gamma - 1$ ), from our measured  $\Gamma = 1.62 \pm 0.27$  at 109.2 days. Since the synchrotron cooling frequency is strongly dependent on the velocity of the outflow, the detection of a cooling break in X-ray monitoring can provide powerful constraints on critical parameters in these models. We thus strongly encourage additional deep *Chandra* X-ray observations of GW170817/GRB170817A toward this end.

#### 4. CONCLUSION

We present late-time *Chandra* observations of neutron star coalescence GW170817/GRB170817A at 109.2 days post-burst, the first sensitive X-ray observations possible since a previous detection at 15.6 days. These data show that the X-ray counterpart has brightened at the same rate as its radio light curve. We show that the X-ray light curve is an excellent match to predictions from outflow models based on radio observations in which the outflow is a cocoon or dynamical ejecta. Our observations thus support a scenario in which both the X-ray and radio emission are the afterglow of an outflow, with-

out requiring a jet that successfully breaks out of the ejecta. Finally, the X-ray brightening strengthens the argument that simple top-hat jet models are not consistent with the latest observations. However, more advanced models of structured jets with off-axis viewing angles should be pursued and cannot yet be ruled out.

Continued *Chandra* monitoring of GRB170817A will be critical for validating the currently-favored outflow model. Since the synchrotron cooling frequency is still above the X-ray emission in this model, additional deep observations by *Chandra* will provide the first indication of the cooling break by detecting a steepening in the X-ray photon index. A detection of the cooling break will provide powerful constraints on the physical parameters of the outflow producing the X-ray and radio emission. Our observations of GW170817/GRB170817A presented here highlight the unique role of *Chandra* in opening the multi-messenger gravitational wave era.

The authors thank Belinda Wilkes and the *Chandra* scheduling, data processing, and archive teams for making these observations possible. This work was supported by Chandra Award Number GO7-18033X, issued by the Chandra X-ray Observatory Center, which is operated by the Smithsonian Astrophysical Observatory for and on behalf of the National Aeronautics Space Administration (NASA) under contract NAS8-03060. J.J.R., M.N. and D.H. acknowledge support from a Natural Sciences and Engineering Research Council of Canada (NSERC) Discovery Grant and a Fonds de recherche du Québec–Nature et Technologies (FRQNT) Nouveaux Chercheurs Grant. J.J.R. and M.N. acknowledge funding from the McGill Trottier Chair in Astrophysics and Cosmology. D.H. acknowledges support from the Canadian Institute for Advanced Research (CIFAR). PAE acknowledges UKSA support.

*Facility:* CXO

## REFERENCES

- Abbott, B. P., Abbott, R., Abbott, T. D., et al. 2017a, *Physical Review Letters*, 119, 161101
- Abbott, B. P., Abbott, R., Abbott, T. D., et al. 2017b, *ApJL*, 848, L12
- Abbott, B. P., Abbott, R., Abbott, T. D., et al. 2017c, *ApJL*, 848, L13
- Abbott, B. P., Abbott, R., Abbott, T. D., et al. 2017d, *Nature*, 551, 85
- Alexander, K. D., Berger, E., Fong, W., et al. 2017, *ApJL*, 848, L21
- Arcavi, I., Hosseinzadeh, G., Howell, D. A., et al. 2017, *Nature*, 551, 64
- Arnaud, K. A. 1996, *Astronomical Data Analysis Software and Systems V*, 101, 17
- Cowperthwaite, P. S., Berger, E., Villar, V. A., et al. 2017, *ApJL*, 848, L17
- Coulter, D. A., Foley, R. J., Kilpatrick, C. D., et al. 2017, *arXiv:1710.05452*
- Drout, M. R., Piro, A. L., Shappee, B. J., et al. 2017, *arXiv:1710.05443*
- Evans, P. A., Cenko, S. B., Kennea, J. A., et al. 2017, *arXiv:1710.05437*
- Fong, W., Berger, E., Blanchard, P. K., et al. 2017, *ApJL*, 848, L23
- Fruscione, A., McDowell, J. C., Allen, G. E., et al. 2006, *Proc. SPIE*, 6270, 62701V
- Goldstein, A., Veres, P., Burns, E., et al. 2017, *ApJL*, 848, L14
- Gottlieb, O., Nakar, E., Piran, T., & Hotokezaka, K. 2017, *arXiv:1710.05896*
- Gottlieb, O., Nakar, E., & Piran, T. 2018, *MNRAS*, 473, 576
- Guidorzi, C., Margutti, R., Brout, D., et al. 2017, *arXiv:1710.06426*
- Haggard, D., Nynka, M., Ruan, J. J., et al. 2017, *ApJL*, 848, L25
- Hallinan, G., Corsi, A., Mooley, K. P., et al. 2017, *arXiv:1710.05435*
- Hjorth, J., Levan, A. J., Tanvir, N. R., et al. 2017, *ApJL*, 848, L31
- Im, M., Yoon, Y., Lee, S.-K. J., et al. 2017, *ApJL*, 849, L16
- Kasliwal, M. M., Nakar, E., Singer, L. P., et al. 2017, *arXiv:1710.05436*
- Lazzati, D., Deich, A., Morsony, B. J., & Workman, J. C. 2017, *MNRAS*, 471, 1652
- Levan, A. J., Lyman, J. D., Tanvir, N. R., et al. 2017, *ApJL*, 848, L28
- Margutti, R., Berger, E., Fong, W., et al. 2017, *ApJL*, 848, L20
- McCully, C., Hiramatsu, D., Howell, D. A., et al. 2017, *ApJL*, 848, L32
- Mooley, K. P., Nakar, E., Hotokezaka, K., et al. 2017, *arXiv:1711.11573*
- Murguia-Berthier, A., Ramirez-Ruiz, E., Kilpatrick, C. D., et al. 2017, *ApJL*, 848, L34
- Nakar, E., & Piran, T. 2017, *ApJ*, 834, 28
- Pian, E., D’Avanzo, P., Benetti, S., et al. 2017, *Nature*, 551, 67
- Piro, A. L., & Kollmeier, J. A. 2017, *arXiv:1710.05822*

- Planck Collaboration, Ade, P. A. R., Aghanim, N., et al. 2016, *A&A*, 594, A13
- Savchenko, V., Ferrigno, C., Kuulkers, E., et al. 2017, *ApJL*, 848, L15
- Schlafly, E. F., & Finkbeiner, D. P. 2011, *ApJ*, 737, 103
- Shappee, B. J., Simon, J. D., Drout, M. R., et al. 2017, [arXiv:1710.05432](https://arxiv.org/abs/1710.05432)
- Smartt, S. J., Chen, T.-W., Jerkstrand, A., et al. 2017, *Nature*, 551, 75
- Soares-Santos, M., Holz, D. E., Annis, J., et al. 2017, *ApJL*, 848, L16
- Troja, E., Piro, L., van Eerten, H., et al. 2017, *Nature*, 551, 71
- Valenti, S., David, Sand, J., et al. 2017, *ApJL*, 848, L24
- Verner, D. A., Ferland, G. J., Korista, K. T., & Yakovlev, D. G. 1996, *ApJ*, 465, 487
- Wilms, J., Allen, A., & McCray, R. 2000, *ApJ*, 542, 914